2nd European Advanced Accelerator Concepts Workshop
13-19 September 2015 *La Biodola, Isola d'Elba*
Europe/Rome timezone

DIAGNOSTIC AND DETECTORS FOR CHARGING AND DAMAGE OF DIELECTRICS IN HIGH-GRADIENT ACCELERATORS

This research was supported by the DoE Phase I grant DE-SC0011347

S.V. Shchelkunov[1,2], T.C. Marshall[1], J.L. Hirshfield[1]

[1]Omega-P, Inc, New Haven, CT 06511, USA; [2]Yale University, New Haven, CT, USA

Research Problem Statement:

- Research is aimed to address issues of a*nalysis of high repetition rate effects in Dielectric Wakefield Accelerators,*

- Specifically,

  to study charging rate and distribution in a thin walled dielectric wakefield accelerator from a passing charge bunch, and

  the physics of conductivity and discharge phenomena leading to damage in dielectric materials useful for accelerator applications.

- The issue is the role played by the beam halo and intense wakefields in charging of the dielectric,

  Not thoroughly studied yet;

  Can lead to undesired deflection of charge bunches and degradation of the dielectric material.

- Plans are to make measurements on a DWA (dielectric wakefield accelerator) system

Approach and Method:

1)

The detector will measure the change in complex electrical conductivity inside the dielectric tubing that is caused by the passage of a charged relativistic electron bunch

Detector is based on measurement of the change of complex admittance of a resonant microwave cavity

Cavity is fitted around the dielectric tubing (that has the complex electrical conductivity.)

2)

The detector can detect permanent damage to the material, and

Transient phenomenon accompanying the passage of one or more charged bunches.

3)

Microwave apparatus was built, and

Signal processing was developed for observing time-dependent electronic charging of dielectric surfaces and/or plasmas.

4)

The test and performance results for a plasma test case will be presented;

in particular, capability to detect small changes ~ 0.1% of a dielectric constant,

which corresponds to the scraping-off of only 0.3nC to the walls of the dielectric liner.

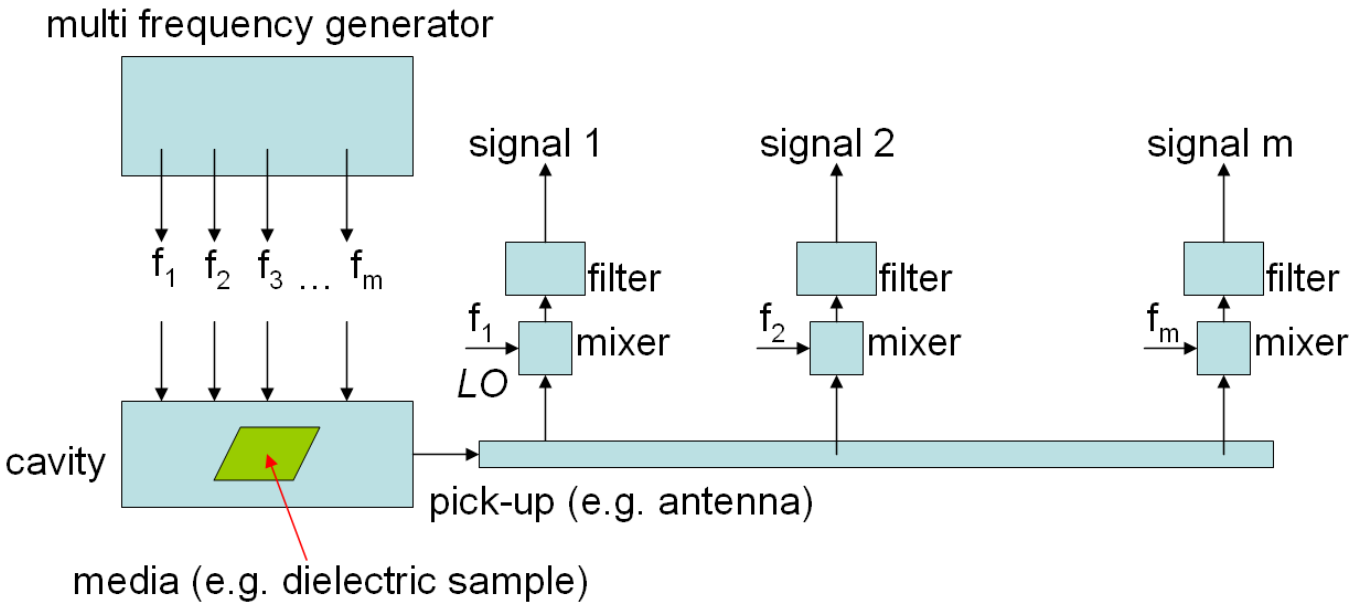

Generic schematic of the measurement system. Only principal elements are shown.

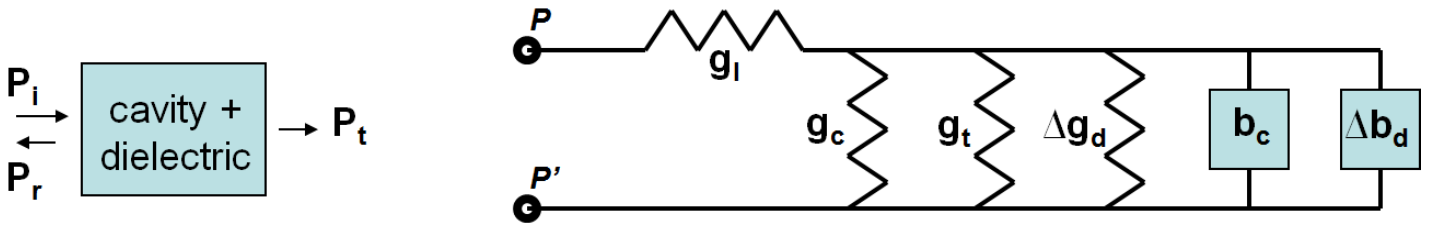

Equivalent circuit for a resonant cavity

Δg_d and Δb_d are the changes in dielectric conductance and susceptance (normalized to the PP'-plane);

g_c and b_c are the cavity conductance and susceptance when the dielectric is not affected by wakefields or halo electrons;

g_l is the conductance of the RF-feeding line and the input coupling;

g_t is the output coupling (assumed to be small);

P_i stands for the incident power; P_t - for the transmitted power; and P_r - for the reflected one.

Using the cavity resonant treatment

$$\frac{P_i}{P_t}\frac{4q_t}{\left[1+\left(1/q_l+1\right)q\right]^2}=1+\frac{\left(1/q_l+1\right)^2}{\left[1+\left(1/q_l+1\right)q\right]^2}\Delta b_d^2\frac{\left(f-F_o'\right)^2}{\left(F_0-F_0'\right)^2}$$

$$q_d+jb_d=\frac{\beta\int\Delta\sigma E^2dv}{\omega_0\varepsilon_0\int E^2dv}$$

where either $g = g_c + g_t + \Delta g_d$ or $g = g_c + g_t$ depending if the dielectric is affected by the halo electrons and wakefields or not, F_0' and F_0 are the cavity resonance frequencies for each respective case, and f is the scanning frequency (frequency of incident RF). β is the cavity coupling. The integrals are taken over the cavity volume, $\omega_0 = 2\pi F_0$, E is the vector electric field, and $\Delta\sigma$ is the change in the complex conductivity

To go further, use

$$Q^2=\frac{\beta^2\left(1/q_l+1\right)^2}{\left[1+\left(1/q_l+1\right)q\right]^2}$$

where Q is the cavity Q-factor

the ratio, $T_m \equiv (P_t/P_i)_m$, for each observer (generator) frequency, f_m

$$T_m = \xi \frac{\left(Q/Q_\xi\right)^2}{1+Q^2\left(2\frac{f_m - F}{F}\right)^2} \cong \xi \frac{\left(Q/Q_\xi\right)^2}{1+Q^2\left(2\frac{f_m - F}{F_\xi}\right)^2}$$

where $\xi = (P_t/P_i)_\xi$ is the transmission (power ratio) when there is no charge present, and similarly, F_ξ and Q_ξ are the resonant frequency and the q-factor respectively. F and Q are the resonant frequency and q-factor when there is a discharge, etc.

$$F = \frac{f_m + f_k}{2} + \frac{F_\xi^2}{f_m - f_k}\frac{T_m - T_k}{\xi}\frac{\xi^2}{T_m T_k}\frac{1}{8Q_\xi^2}$$

$$\frac{1}{Q^2} = \frac{\xi}{T_k}\frac{1}{Q_\xi^2} - \left(\frac{f_m - f_k}{F_\xi} + \frac{F_\xi}{f_m - f_k}\frac{T_m - T_k}{\xi}\frac{\xi^2}{T_m T_k}\frac{1}{4Q_\xi^2}\right)^2$$

STEP #1

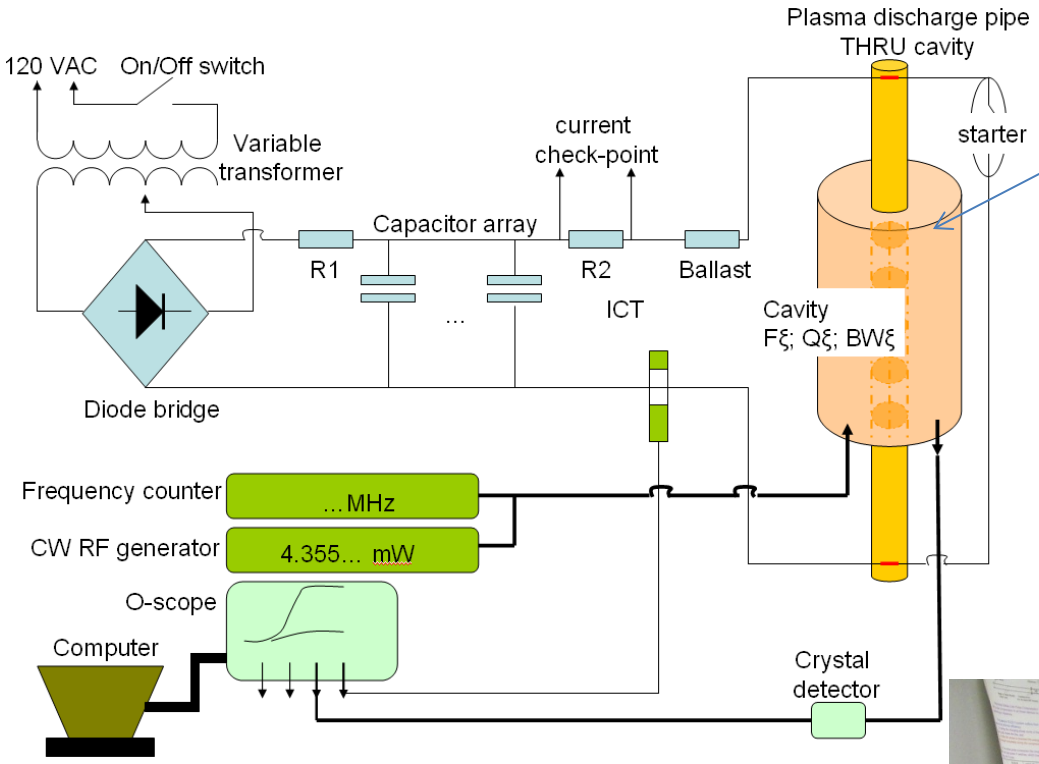

F_ξ = 2479.157 MHz,
Q_ξ = 1175, and
$BW_\xi = F_\xi / Q_\xi$ =2.11 MHz

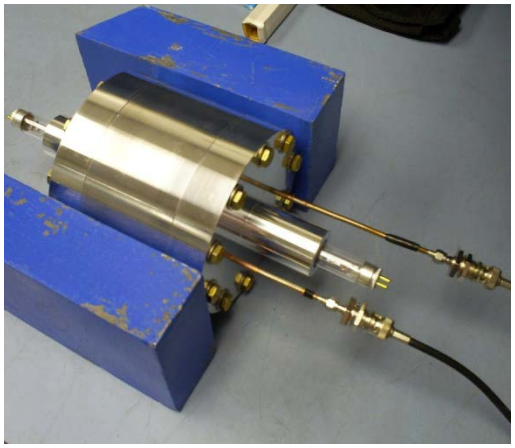

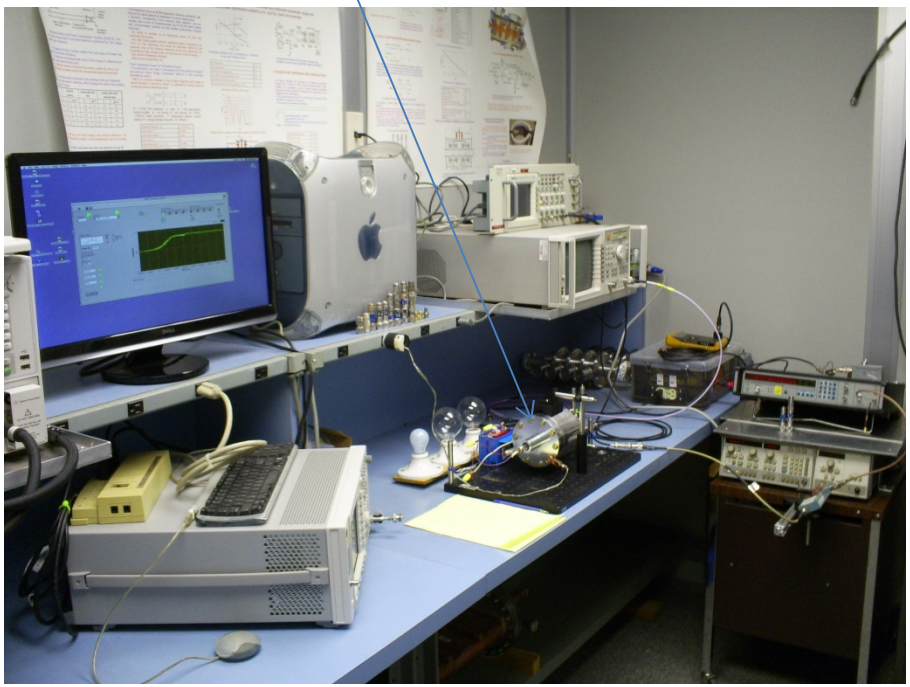

Diagram of the experimental setup: to record three different traces, the probing frequency (of the CW RF generator) was adjusted, and the discharge event was repeated.

Choice 1: $f_1 \approx F_\xi$; $f_2 \approx F_\xi + (BW_\xi/2)$ and $f_3 \approx F_\xi + BW_\xi$,

Choice 2: $f_1 \approx F_\xi - (BW_\xi/2)$; $f_2 \approx F_\xi$ and $f_3 \approx F_\xi + BW_\xi/2$

Current behavior during the time when microwave signals are observed.

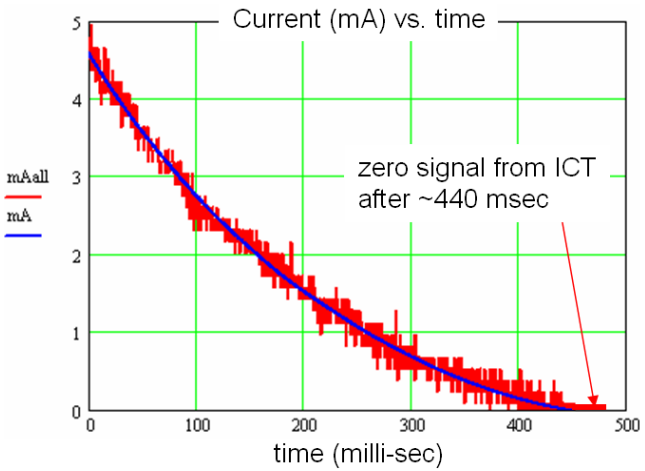

Microwave signals transmitted through the resonator which is loaded with plasma, using three different frequencies.

Traces were recorded at three observer frequencies:

f1 = 2479.1936 MHz (≈ resonant frequency) (RED)
f2 = 2480.276 MHz (BLUE)
f3 = 2481.141 MHz (BROWN)

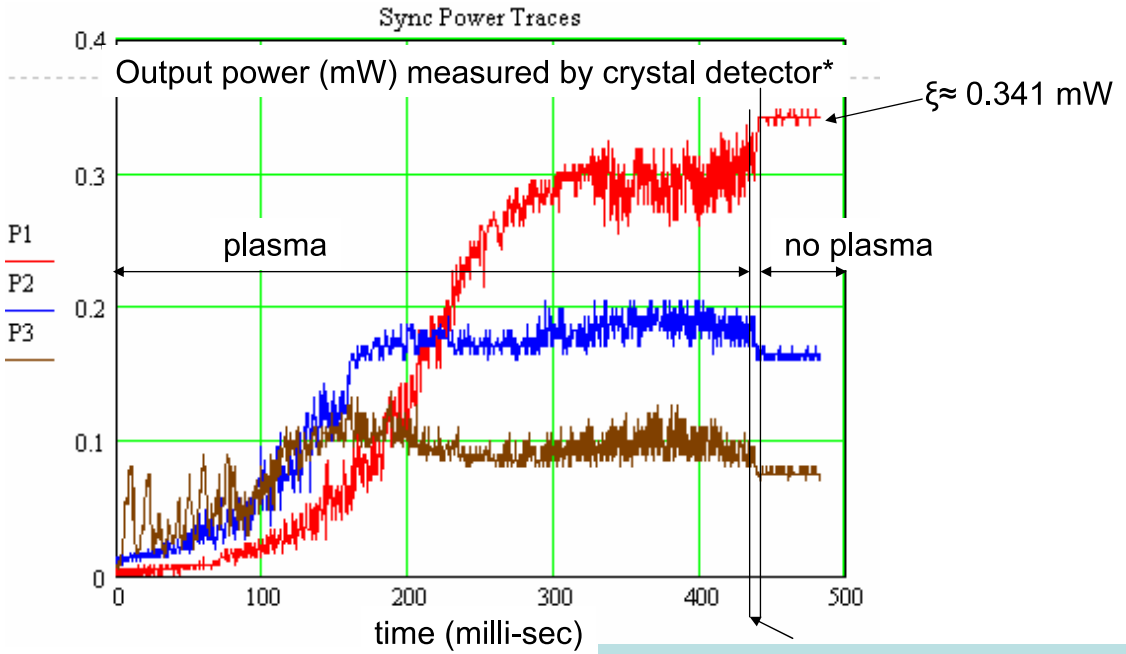

*Input power stays the same

This "jump" in the traces data points will give us our sensitivity

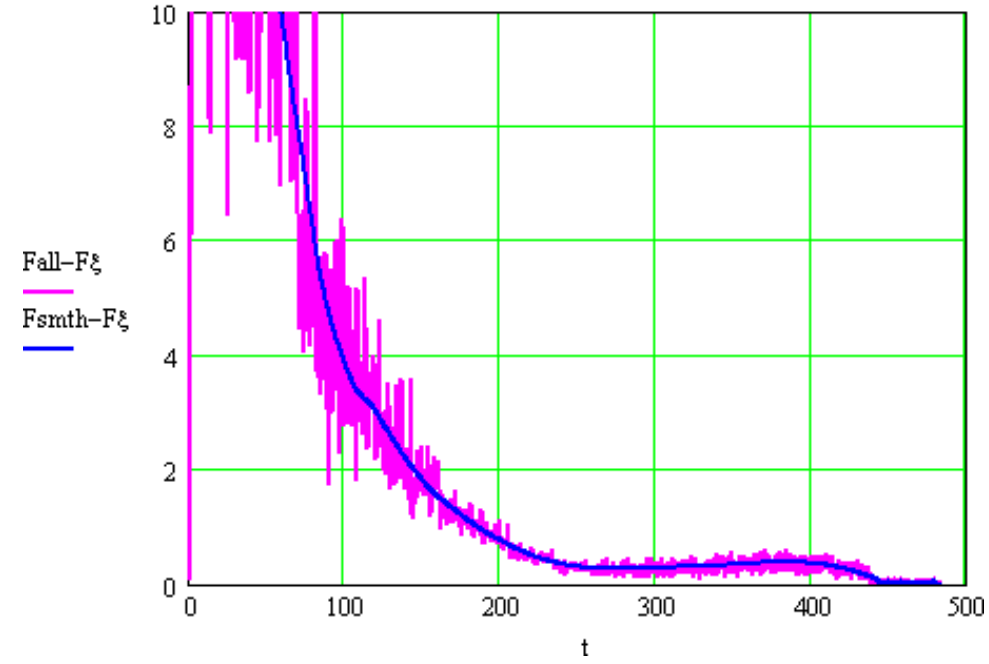

Changes in the resonant Frequency (MHz) vs. Time (ms)

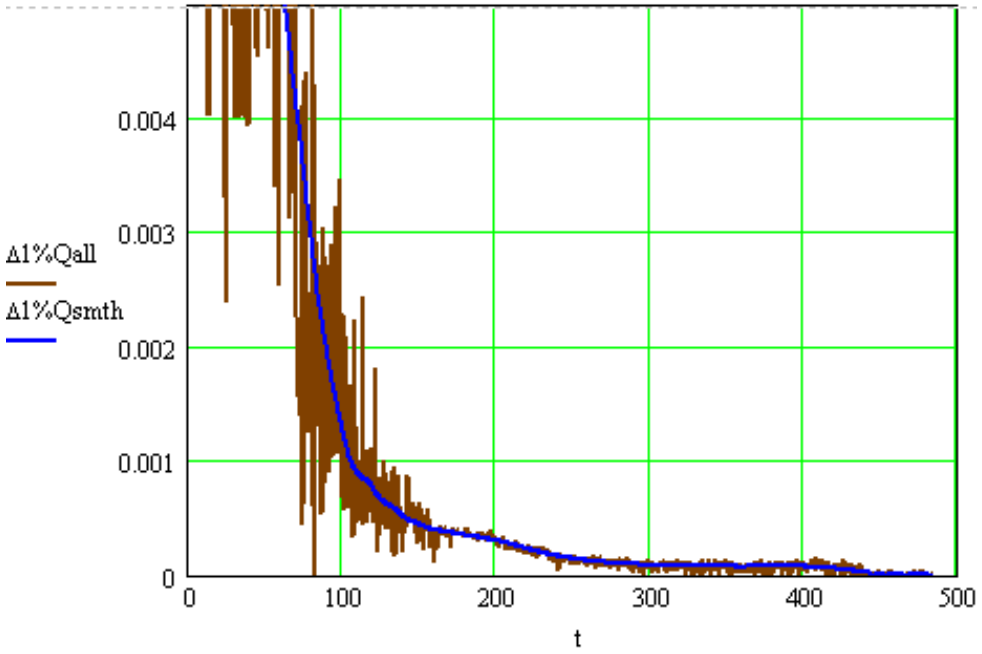

Changes in the Q-factor vs. Time (ms).

This is plotted as (1/Q-1/Q_ξ), where the latest in the Q-factor when there is no plasma

$$\frac{\Delta\varepsilon}{\varepsilon} = 1 + A\frac{F - F_\xi}{F_\xi} + B\left(\frac{F - F_\xi}{F_\xi}\right)^2 + \ldots$$

$$\Delta(loss\tan) = C\left(\frac{1}{Q} - \frac{1}{Q_\xi}\right)\left(1 + D\frac{F - F_\xi}{F_\xi} + E\left(\frac{F - F_\xi}{F_\xi}\right)^2 + \ldots\right)$$

$$\varepsilon_{\mathrm{Im}} = \varepsilon_{\mathrm{Re}} \cdot loss\tan$$

Expand the complex dielectric constant in a power series

To find the coefficients A, B, … and E we will

* use e.g. HFSS,

* do simulations having changes in the medium ε, and loss-tan, and find the corresponding changes in the cavity's frequency and Q-factor.

* once the dependences are found, we reverse them

STEP #2

Example:

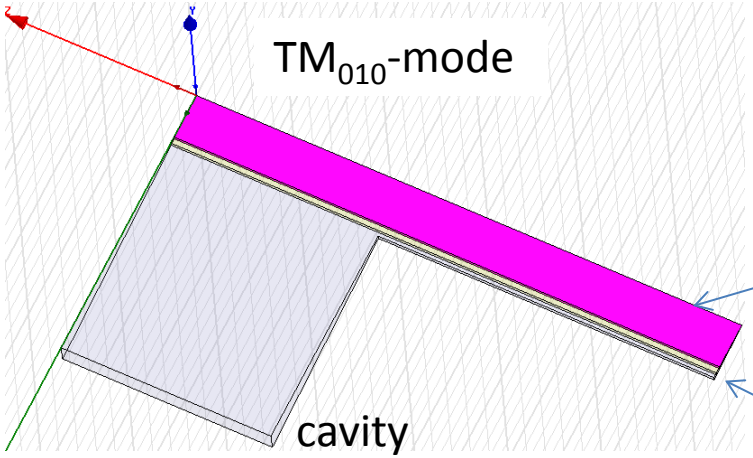

$$\frac{\Delta\varepsilon}{\varepsilon_{ini}} = 1 + (-22.5579)\frac{F - F_\xi}{F_\xi} + (-5.4125\cdot 10^{-4})\left(\frac{F - F_\xi}{F_\xi}\right)^2$$

$$\Delta(loss\tan) = (11.3047)\left(\frac{1}{Q} - \frac{1}{Q_\xi}\right)\left(1 + (22.5814)\frac{F - F_\xi}{F_\xi} + (648.7763)\left(\frac{F - F_\xi}{F_\xi}\right)^2\right)$$

$$\varepsilon_{\mathrm{Im}} = (11.3047)\left(\frac{1}{Q} - \frac{1}{Q_\xi}\right)$$

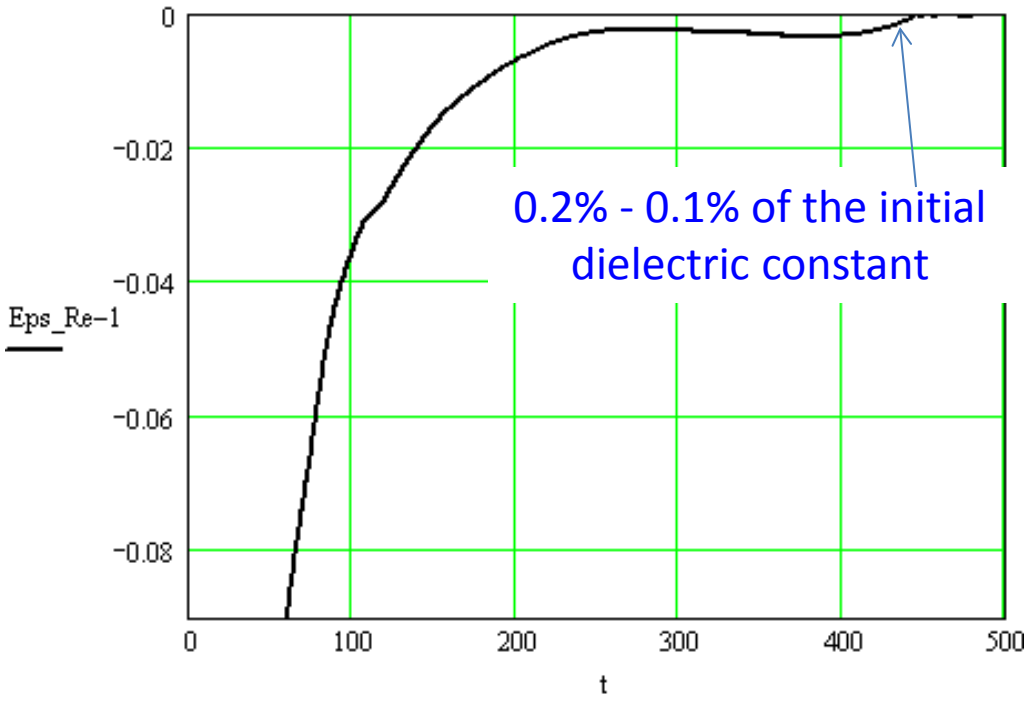

Changes in Real part of dielectric constant vs. Time (ms)

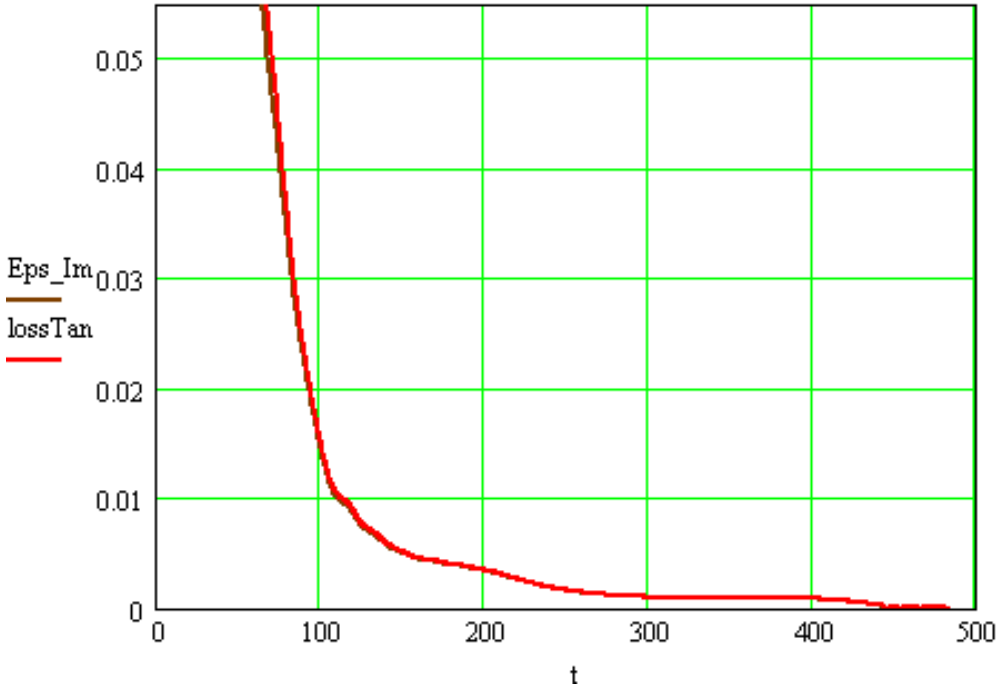

Changes in the loss-tan and the Imaginary part of dielectric constant vs. Time (ms)

To find corresponding changes in the density of free electrons, we will use reasonable assumption about our medium under test

STEP #3

For instance for the case described here, we also can use well known relationships between the density of free electrons, n_e, and their collision frequency, F_{coll} and the plasma dielectric constant $\varepsilon_0(\varepsilon_{\mathrm{Re}} + j\varepsilon_{\mathrm{Im}})$

$$\varepsilon_{\mathrm{Re}} = 1 - \frac{n_e \cdot e^2}{m_e \varepsilon_0 \left(2\pi F_\xi\right)^2} \frac{1}{1 + \left(F_{coll} / F_\xi\right)^2}$$

$$\varepsilon_{\mathrm{Im}} = \frac{n_e \cdot e^2}{m_e \varepsilon_0 \left(2\pi F_\xi\right)^2} \frac{F_{coll} / F_\xi}{1 + \left(F_{coll} / F_\xi\right)^2}$$

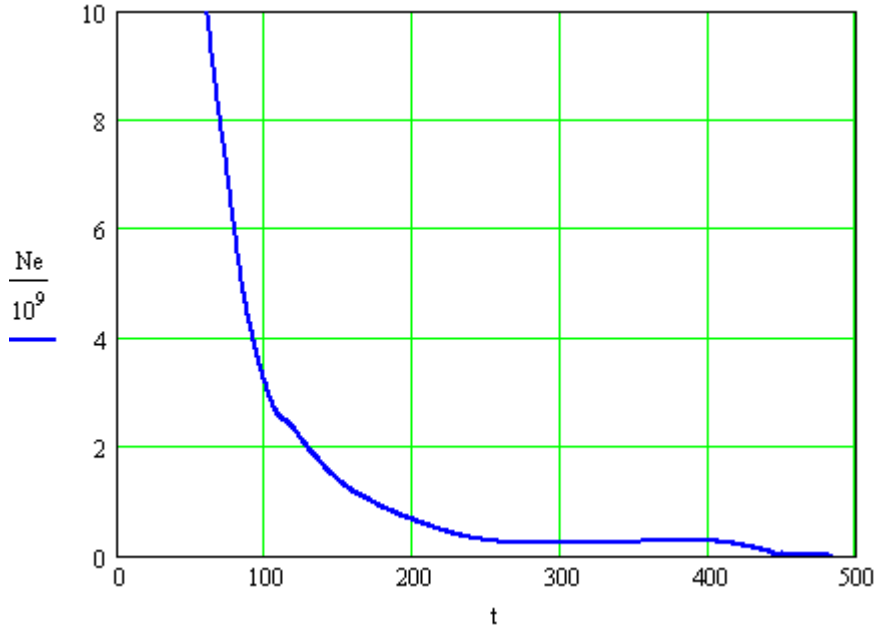

Electron density ($\times 10^9$ cm^{-3}) vs Time

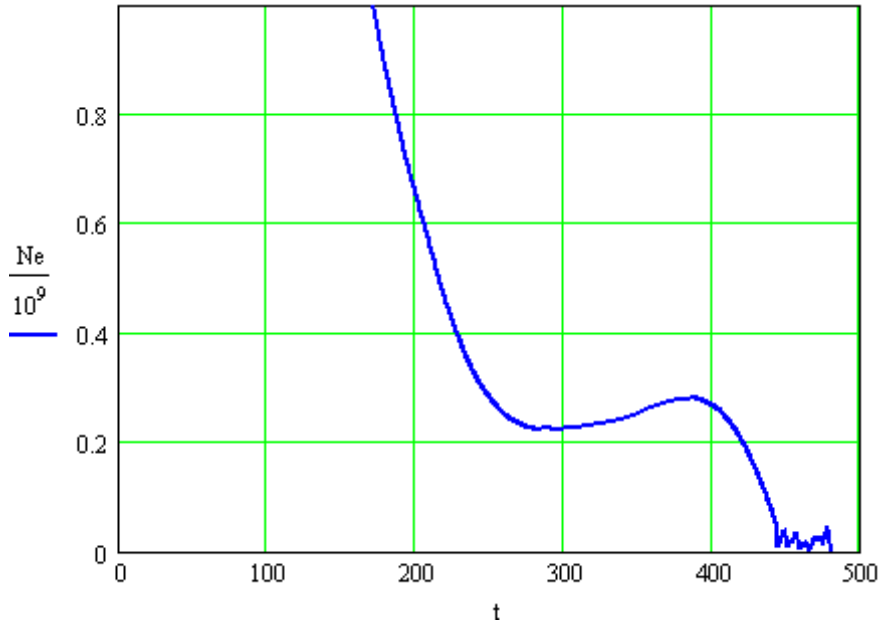

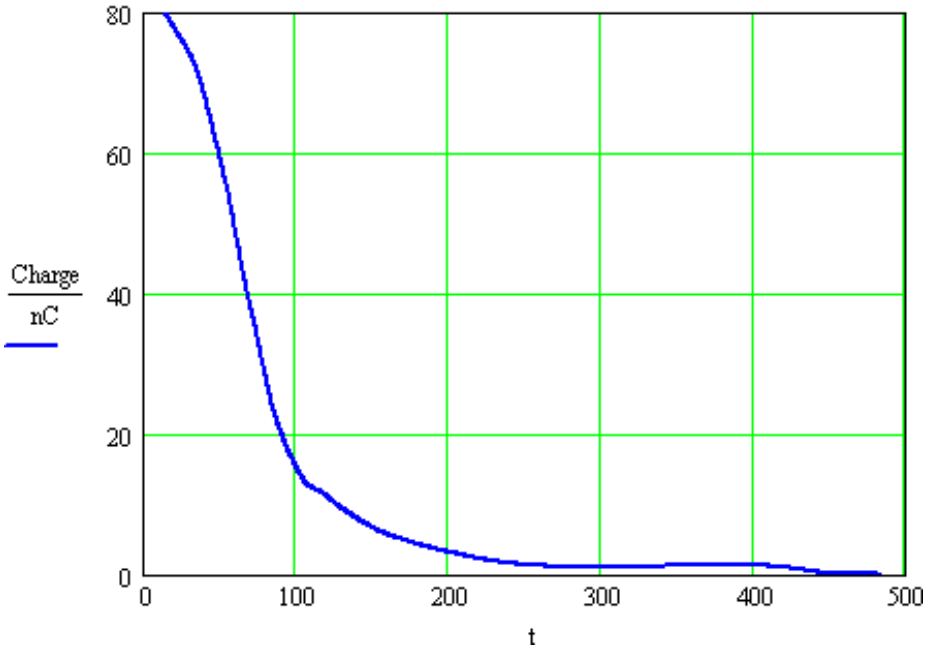

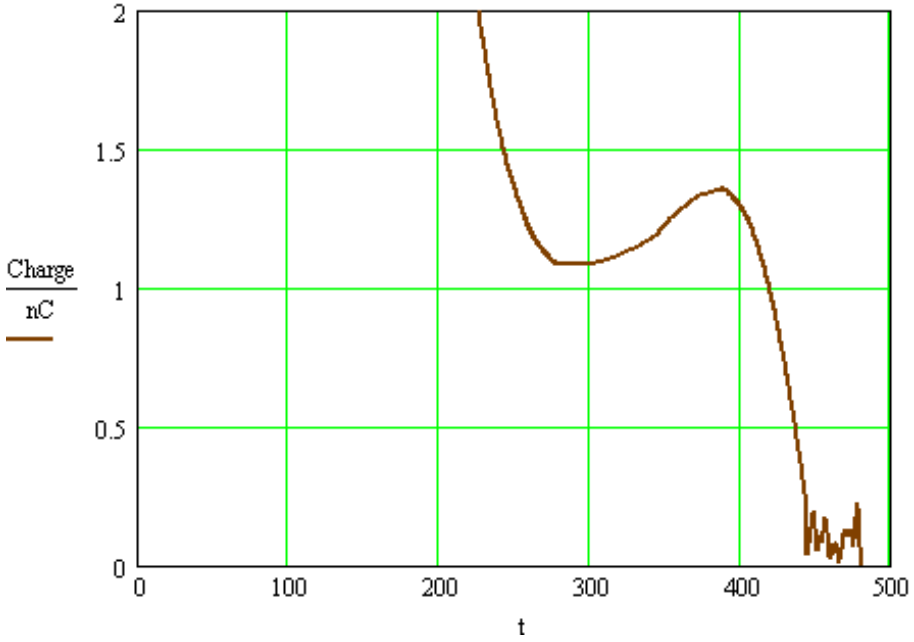

Charge (nC) vs. Time (ms)

few Conclusions

- **can detect the densities at or even above 10^{10} cm^{-3} [50- 60 nC]**
- **can detect electron density at or even below ~ 10^{8} cm^{-3} [0.5 nC]**
- **dynamic range ~20 dB [for our simple, not sophisticated, setup]**

few Considerations

- The upper limit will be greater when a more powerful RF generator and more sensitive detectors (and output amplifiers) are employed.
- The lower limit can be improved by increasing the cavity Q-factor. This follows from $N_e \sim BW_\xi$ at low densities of free electrons. E.g.:

  In our present setup has Q ~1000, and the minimum charge $N_{e,\,min}$ ~ 0.5 ***n***C [10^{8} cm^{-3}]

  Q ~3000 will still allow us to capture the processes on the ***micro***-sec time-scale, yet the min. change ~ 0.15 ***n***C [3÷4 × 10^{7} cm^{-3}]

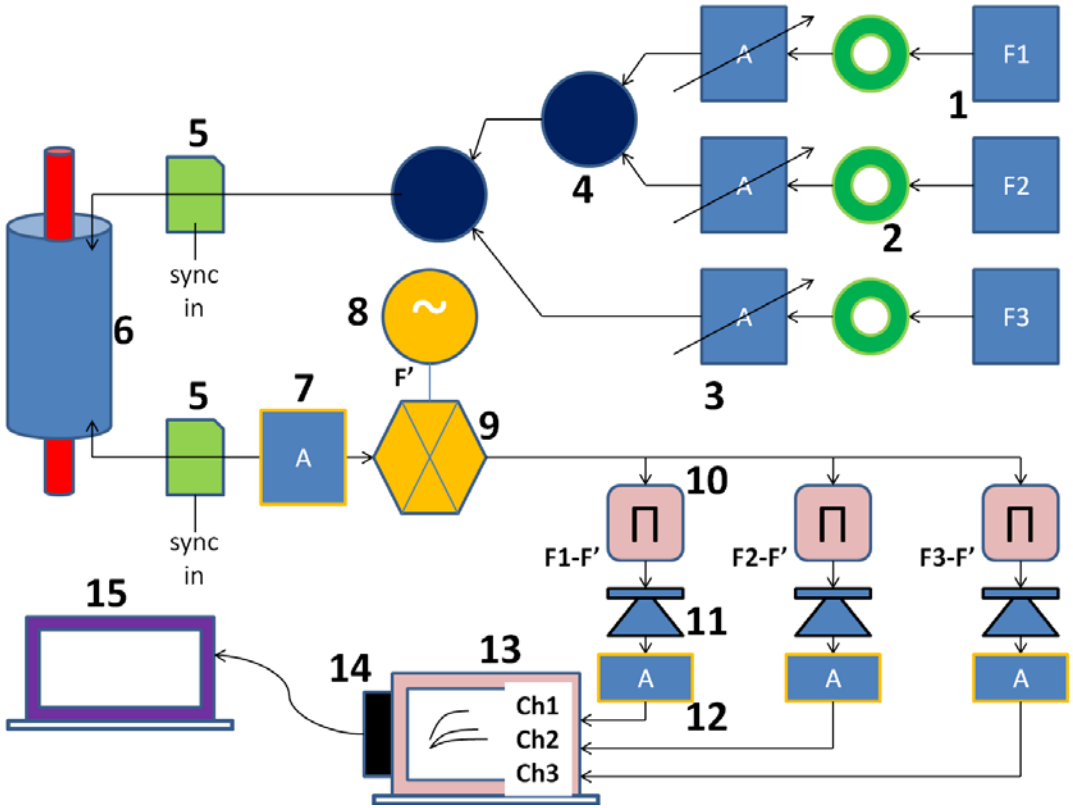

Diagram of a detector to install at an accelerator: 1 – tunable frequency generators (3x); 2 - circulators (3x); 3 – variable amplifier (3x); 4 – power combiners (2x); 5 – fast RF switches (2x); 6 – cavity with samples under test; 7 – high frequency output amplifier; 8 – local oscillator; 9 – mixer; 10 – band-pass frequency filters (3x); 11 – crystal detectors (3x); 12- low frequency amplifiers (3x); 13 – oscilloscope; 14 – GPIB/USB-Ethernet/USB adapter; 15- computer.

Dielectric constant and loss-tan of Quartz (pure**) and Alumina (**99.6% pure**) near 2.5 GHz**

Samples were ordered from two manufacturers: http://technicalglass.com and http://advaluetech.com.

The quartz samples were either 13×15 mm or 12×16mm (ID×OD); the alumina samples were either 9.51 × 13.02 mm or 9.585 × 12.91 mm. We denote these samples by following code–names: Q13:15, Q12:16, A9.51:13.02, and A9.59:12.91.

Sample	Material	Changes in Frequency (MHz)	Changes in 1/Q	Dielectric constant**	Loss-tan***
Q13:15	Quartz	-83.57	*	3.408	$< 1 \times 10^{-5}$
Q12:16	Quartz	-162.67	*	3.391	$< 1 \times 10^{-5}$
A9.51:13.02	Alumina	-313.06	3.86×10^{-4}	8.731	1.38×10^{-3}
A9.59:12.91	Alumina	-289.28	2.85×10^{-4}	8.023	1.09×10^{-3}

* cannot be measured within the measurement accuracy;

** $\Delta\varepsilon = 6 \times 10^{-3}$;

***$\Delta(losstan) \leq 1 \cdot 10^{-5}$ (for Quartz); and $\Delta(losstan) \leq 5 \cdot 10^{-5}$ (for Alumina)

Bibliography:

[1] S.C. Brown, "Basic Data of Plasma Physics", The Technology Press and John Wiley & Sons, New York (1959); see pp. 17-23.

[2] Vladimir D. Shiltsev, FERMILAB-PUB-12-100-APC (2012).

[3] M. Thompson, H. Badakov, A. Cook, J. Rosenzweig, T. Tikhoplav, I Blumenfeld, M. Hogan, I. Ischebeck, and N. Kirby, Phys. Rev. Lett. **100**, 214801 (2008).

[4] C. Li, W. Gai, C. Jing, J.G. Power, C.X. Tang, and A. Zholents, Phys. Rev. ST – Accel. Beams **17**, 091302 (2014).

[5] G.V. Sotnikov, T.C. Marshall, and J.L. Hirshfield, Phys. Rev. ST Accel. Beams, **12**, 061302 (2009).

[6] G.V.Sotnikov and T.C. Marshall, Physical Review ST-Accel. Beams **14**, 031302 (2011); see also C. Jing, A. Kanareykin, J.G. Power, M. Conde, Z. Yusof, P. Schoessow, W. Gai, Phys. Rev. Lett. **98** 144801, (2007).

[7] Lawrence Gould and Sanborn C. Brown, J. Appl. Phys. **24**, 1053 (1953).

[8], [9], [10] S.C. Brown and D.J. Rose, **23**, 711 (1952); 719 (1952); 1028 (1952).

[11] J.C. Slater, Rev. Mod. Phys. **18**, 481 (1946)

[12] P. Schoessow, "Charging and Radiation Damage Effects in Dielectric Wakefield Structures", at 2nd Workshop on Applications of Dielectric Wakefield Structures to Next Generation X-Ray Free Electron Laser Facilities, Los Alamos NM, December 5-6, 2013 (Euclid Techlabs). http://dwa.lanl.gov/talks/los%20alamos%20%20workshop%20Schoessow.pdf

2nd European Advanced Accelerator Concepts Workshop

13-19 September 2015 *La Biodola, Isola d'Elba*
Europe/Rome timezone